NPL

NPL REPORT AS 90

Global NanoMappp Report: Physico-Chemical Properties of NM 302 Nano-silver Reference Material

Kenneth Robinson, Ratna Tantra , Tony Fry, Dimitris Sarantaridis, Dipak Gohli, Crispin Allen, Paul Quincy, Caterina Minelli

JULY 2014

Global NanoMappp Report: Physico-Chemical Properties of NM 302 Nano-silver Reference Material

Kenneth Robinson, Ratna Tantra, Tony Fry, Dimitris Sarantaridis, Dipak Gohli, , Crispin Allen, Paul Quincy, Caterina Minelli
Analytical Science and Material Divisions, NPL

ISSN: 1754-2928

National Physical Laboratory
Hampton Road, Teddington, Middlesex, TW11 0LW

Approved on behalf of NPLML by Dr Alex Shard, Principle Research Scientist.

CONTENTS

1. INTRODUCTION

Nanomaterials are now used extensively in a wide range of applications and consumer products and are of increasing environmental concern. Understanding particle behaviour in the environment and within organisms is a prerequisite to understanding their bioavailability and toxicity.

This had led to our involvement in PROSPEcT and the global initiative spearheaded by the OECD. Our activities in PROSPEcT involved the characterisation of different properties of nano-ZnO (NM 110, NM 112 & NM 113) and nano-CeO_2 (NM 211, NM 212 & NM213). Our initial study, in collaboration with University of Exeter, had shown that the acute toxicity of nano-ZnO is similar to bulk and soluble forms of the metal oxides/metal.[1]

This report will present physicochemical data associated with colloidal silver, NM 302, under the Global NanoMappp initiative. It is an extension of our work post PROSPEcT and NM-302 can be further considered as potential test materials under the JRC library of reference materials.

2. MATERIALS AND PROTOCOLS

2.1 MATERIALS

NM 302 was supplied by Fraunhofer with the following information; each NM 302 sample vial contains 2000 mg of silver nanomaterial dispersion. This consists of elongated Ag nanorods (8.6% w/w, ≥99% purity), with widths of 100 – 200 nm and lengths of 5 - 10 µm, dispersed in an aqueous solution containing polyvinylpyrrolidone (<1% w/w), acrylic/acrylate copolymer (< 2% w/w) and polycarboxylate ether (< 2% w/w). Unless stated otherwise all water used was deionised with a resistivity of 18.2 MΩ

2.2 PROTOCOLS

2.2.1 NM 302 sample preparation

In the as received state the dispersions were completely sedimented, and would return to this state within minutes of any attempted redispersion; therefore it was necessary to dilute samples significantly to obtain sufficient sample stability for testing. The colloidal nanomaterial was diluted to a concentration of 50 mg/L to obtain suitable stability. To preserve all other aspects of the sample dispersion it was necessary to ensure the medium remained the same, hence dilution was only carried out using nanoparticle-free NM 302 dispersant.

To obtain the nanoparticle-free NM 302 dispersant, the liquid from multiple sample vials was extracted via syringe and passed through a 0.1um syringe filter into clean 2 ml centrifuge tubes, the filtered dispersant was then spun at 6000 rpm in a Eppendorf centrifuge 5430 (Eppendorf, Germany) for 15 minutes, the supernatant extracted and then passed thought another 0.1 syringe filter into a pre-cleaned glass vial. This was repeated multiple times to obtain the required volume of dispersant. The effectiveness of this procedure was tested via Dynamic Light Scattering, which showed the presence of ~ 1.5 nm particles, most likely due to the organic components present in the dispersant.

50 mg/L dispersions were made by weighing 6 mg of the as received dispersion from a sample vial that had been vortexed from 5 minutes, into an amber glass vial. This was then diluted by addition of 10 mL of the nanoparticle-free dispersant. Vortexing was used to disperse the nanomaterial in all cases as more intense methods such as sonication would run the risk of breaking up the primary particles.

Unless stated otherwise all measurements were carried out on these 50 mg/L dispersions.

2.2.2 Differential centrifugal sedimentation (DCS).

DSC measurements were taken with a CPS Disc Centrifuge DC 20000 (CPS, USA), the centrifugal disc was run at 20000 rpm and a density gradient of aqueous sucrose solution (8% to 24% wt/wt),

capped with a 0.5ml dodecane layer to prevent evaporation, was built up and allowed to equilibrate for 30 minutes. Six dispersions were tested in triplicate by injecting 100 µL at a time into the instrument. A calibration standard consisting of 0.223 µm PVC particles (Analytik, UK) was injected before each sample injection to ensure measurement accuracy. As the particles are elongated rods a non sphericity factor of three was applied to the measurements in the instrument software to correct for shape effects.

2.2.3 Scanning electron microscopy (SEM)

A vial of NM 302 was lightly vortexed for 5 minutes to ensure thorough mixing of the sedimented contents. Immediately afterwards 1mL of the sample was extracted via pipette and deposited onto the surface of a section of clean silicon wafer. The wafer was left to incubate for 5 minutes at room temperature before being dip rinsed in a beaker of DI water to remove excess nanomaterial and salts. The wafer was then dried under vacuum for an hour to remove any remaining liquid, after which it was attached to an aluminium mount via a conductive carbon adhesive disk and placed in the SEM instrument for imaging. The SEM was calibrated using a SIRA grid calibration set (SIRA, UK). These are metal replicas of cross ruled gratings of area of 60 mm^2 with 19.7 lines/mm for low magnification and 2160 lines/mm for high magnification calibrations, accurate to 0.2 %

SEM imaging was carried out on a Supra40 Microscope (Zeiss, Germany) at a working distance of 8.4mm with a 0^o tilt angle. Images were acquired using the SE2 lens operating at 5 kV at various magnifications; for particle sizing the magnification was fixed at 10k.
Particle size distributions were obtained by analysing the SEM images using the ImageJ software (NIH, USA). The polygon selection tool was used to trace the outline of the particles for measurement. Particles whose outlines were obscured by others were omitted from the analysis, with the exception of when the outline could be reliably inferred, e.g. two nanorod bisecting each other.

2.2.4 Dynamic light scattering (DLS)

DLS size measurements were carried out with a Zetasizer Nano ZS (Malvern Instruments, USA) using ZEN 0118 disposable low volume cuvettes with a cap fitted (Malvern Instruments, USA). The accuracy of the instrument was checked using 100 nm latex particles (NIST, USA). Samples were allowed to equilibrate at 25 °C in the instrument for 2 minutes before measurement. Triplicate measurements of six dispersions were carried out, with each measurement consisting of 10 repeats lasting 30 seconds each. Due to the presence of additives in the NM 302 dispersant the viscosity was significantly higher than water, as this has a large effect on DLS particle size, viscosity measurements were obtained using a AR-G2 Rheometer (TA Instruments, USA) giving a value of 8.48 mPa.S.

2.2.5 Scanning mobility particle sizing (SMPS)

Solutions of nano-rods were prepared (ca. 100 mg of sample in 40 mL DI water), with the respective aerosols generated using a nebuliser (3.5 L/minute clean air flow). The aerosols were in turn fed through a dryer before reaching the electrostatic classifier (TSI 3080 with Kr-85 bipolar charger, TSI, USA) and the Differential Mobility Analyser (TSI 3081, TSI, USA). For every distinct size bin created by the classifier and DMA, the particle number concentration was measured using a Condensation Particle Counter (TSI 3775, TSI, USA).

2.2.6 X-ray diffraction (XRD)

X-ray diffraction traces were obtained using a Siemens D5000 diffractometer. This consisted of a theta-theta goniometer and an NPL specimen stage. The X-ray source used for these measurements was the Cu-Kα X-ray (40 kV, 30 mA); a Ni filter was used to remove the Cu-Kβ component of the X-ray. The X-ray optics consisted of a 0.6 mm anti scatter slit, a 1 mm collimation slit and a 1 mm detector slit. The diffraction measurement was conducted using coupled theta-theta drives in standard Bragg-Brentano geometry. The data was collected over a 2-theta range of 3° to 140° using a step size of 0.010° and a count time of 1.5 s/step. The diffracted data was electronically collected and stored on

the laboratory PC. Prior to the measurement, the X-ray beam was aligned by placing the X-ray source and the detector in line and passing the X-ray beam through a glass slit, the direct beam was attenuated using copper foil placed in front of the detector. Having aligned the two drives and the stage height a standard reference material (corundum) was used to check the alignment over a range of 2-theta values. Having collected the full diffraction trace the Scherrer equation was used to evaluate the crystallite size.

2.2.7 Zeta potential

Electrophoretic measurements were obtained using a Zetasizer Nano ZS (Malvern Instruments, USA) equipped with a 633 nm wavelength laser. DTS1235 zeta-potential standard (Malvern Instruments, USA) was used to qualify the performance of the instrument. Sample preparation involved the filling of a DTS1070 disposable capillary cell (Malvern Instruments, USA). Prior to their use, these cells were thoroughly cleaned with ethanol and de-ionised water, as recommended by the instrument vendor. For analysis, the individual cell was filled with the appropriate sample and flushed before re-filling; measurements were carried out on the second filling. The dispersions were allowed to equilibrate in the instrument at 25 °C for 2 minutes before measurement. Measurements were carried out on six dispersions in Auto mode, and typically consisted of 12 repeats. Malvern Zetasizer Software (v7.10) was used for data analysis, and zeta-potential values were estimated from the measured electrophoretic mobility data using the Smoluchowski equation.

2.2.8 Turbidity

Turbidity was measured using Micro100 RI turbidity meter (HF Scientific, USA); this meter has an infrared light source that meets the international standard ISO 7027 for turbidity measurements. The meter was calibrated on standards which are based on AMCO-AEPA-1 microspheres; these standards are traceable to standard formazin suspension. Standard values of 1000, 10 and 0.02 NTU were used to calibrate the meter. Prior to use, the meter was allowed to warm up for 30 minutes. Sample cuvettes (HF Scientific, USA) were used to hold the sample. Note that glass thickness may vary between cuvettes, and also within the same cuvette. Hence, individual vials were indexed by finding the point of the cuvette in which light passes through to give the lowest reading; once indexed the holder was marked accordingly. Prior to their use, cuvettes were cleaned, in accordance to manufacturer's instructions. This involved washing the interior and exterior of the cuvette with a detergent (2% Hellmanex in DI water); it was then rinsed several times in distilled water before finally rinsing in DI water. The cuvette was placed into the meter and signal allowed to settle for 5 minutes before taking readings.

2.2.9 Redox potential

The redox potential of the NM302 dispersion was measured using an ORP Testr (Oakton Instruments, USA). This measures the potential difference across two electrodes: a Pt electrode against a double junction Ag/AgCl reference electrode. The electrode was used according to the manufacturer's instructions. Prior to use the electrode was pre-conditioned in clean tap water for 30 minutes before rinsing in distilled water. The ORP electrode was calibrated using a Zobell ORP Calibration Solution (YSI, USA). The measured redox potential value for the Zobell solution was 237 mV at 21.6 °C; this was compared to the literature value of 238 mV at 22.0 °C and the instrument adjusted accordingly. When making measurements, the electrode was carefully placed in a vial containing the sample; with sufficient liquid sample to cover the sensing element. The electrode was carefully stirred a little and then placed in a fixed position, slightly above the bottom of the container. The signal output was allowed to settle for 5 minutes before a reading was taken and the measured potential and temperature of solution noted. After measurement, the electrode was cleaned with tap water and final rinse was with distilled water, after which further measurements could be made. A correction value of +206 mV was applied to all measurements to allow comparison to the Standard Hydrogen Electrode.

2.2.10 Reactive oxygen species (ROS)

Six 1 mL NM302 dispersions containing 0.1 mol/L KI (Sigma Aldrich, USA) were made by adding 100 µL of freshly prepared 1 mol/L KI solution to 900 µL of sample. Additionally, two sets of six samples containing 0.1 mol/L KI in NM302 dispersant and 50 mg/L NM302 respectively were prepared as negative and positive controls; All samples were made in individually capped disposable UV transparent absorption cells and irradiated using a M-20 Benchtop Transilluminator (UVP, USA) operating with a peak wavelength of 302 nm The cells were placed horizontally on the transilluminator surface with the clear sides of the cell facing down to ensure maximum UV transmission into the samples. The samples were subjected to 10 minute periods of irradiation, followed by 5 minute periods of non-irradiation to reduce sample overheating. The samples containing nanomaterials were transferred to centrifuge tubes and spun at 20800 rcf for 15 minutes and the supernatant collected for analysis by UV-visible spectroscopy. Sample solutions were transferred to capped disposable UV adsorption cells and UV-visible absorbance spectrum was acquired. Absorption spectra were acquired with a Lambda 850 UV-Vis spectrometer supported by UV Winlab software [Version 5.1.5] (Perkin Elmer, USA). The instrument wavelength calibration was checked using a 15246-Ho Holmium glass standard (Serial # 9392, Starna Scientific, UK). For the reference channel of the spectrophotometer, a matched cell containing the corresponding dispersing media with no nanoparticles was used. Absorbance scans from 300 nm to 500 nm were performed, using a slit width of 2 nm and a scan rate of 50 nm/min. Optical absorbance at 352 nm was specifically noted

3 RESULTS

3.1 PARTICLE SIZE

3.1.1 Differential centrifugal sedimentation (DCS)

DCS works by measuring the time it takes for injected particles to move from the centre of a spinning disc to the edge where they are detected using a turbidity detector; the larger the particle (for a given density) will mean the shorter the time to reach the edge. One limitation of this technique is that it requires the density of the particle to be accurately known, including any coatings or adsorbed analytes on the surface. As density information for the particles was not supplied with the material for the purposes of this study NM 302 was assume to have the same density as silver (10.49 g/cm).

Table 1: DCS particle diameter distribution statistics for six NM 302 dispersions (Batch # 06212).

	Particle Diameter Distribution (nm)								
Sample	**Absorption**				**Number**				**PDI**
	Mean	**D_{10}**	**D_{50}**	**D_{90}**	**Mean**	**D_{10}**	**D_{50}**	**D_{90}**	
1	363	246	350	492	279	188	268	382	1.25
2	369	252	357	496	287	195	276	392	1.25
3	372	256	361	497	291	197	280	397	1.24
4	361	249	350	484	283	195	273	386	1.24
5	367	250	353	494	286	197	274	388	1.24
6	365	251	352	489	287	200	277	388	1.23
Mean	366	251	354	492	286	195	275	389	1.24
±σ	3.44	3.16	3.90	4.57	3.73	3.68	3.73	4.71	0.01
RSD (%)	0.94	1.26	1.10	0.93	1.31	1.88	1.36	1.21	0.52

DCS results (Table 1) show NM302 to be polydisperse, with a broad distribution with a mean particle diameter of 366 ± 3.44 nm (adsorption) and 286 ± 3.73 nm (number), and an average Polydispersity Index (PDI) of 1.24 ± 0.01; PDI here is calculated as the mean particle size $_{(weight)}$ / mean particle

size$_{(number)}$. It should be noted that preliminary DCS measurements showed no large particles >1µm so subsequent measurements were only run to this diameter.

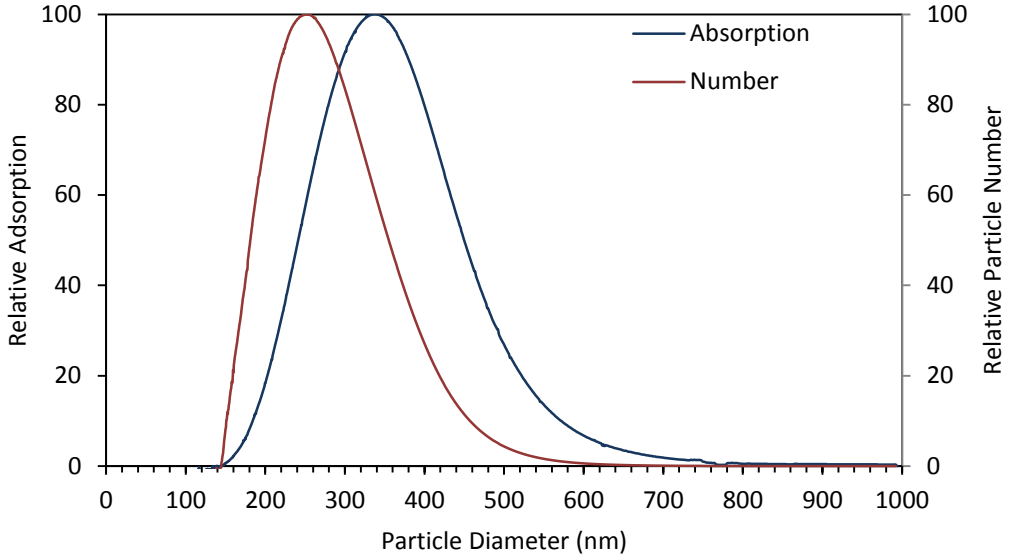

Figure 1: Averaged DCS adsorption and number particle diameter distributions for six NM 302 dispersions. Each dispersion was measured was measured in triplicate.

The averaged size distribution plots for NM 302 (Fig 1) show peak maxima at 340 nm (adsorption) and 251 nm (number). The particle diameters obtained via DCS are more in agreement with the manufacturer's values for particle width, implying that the particles are generally travelling through the DCS gradient tip first.

3.1.2 Scanning electron microscopy (SEM)

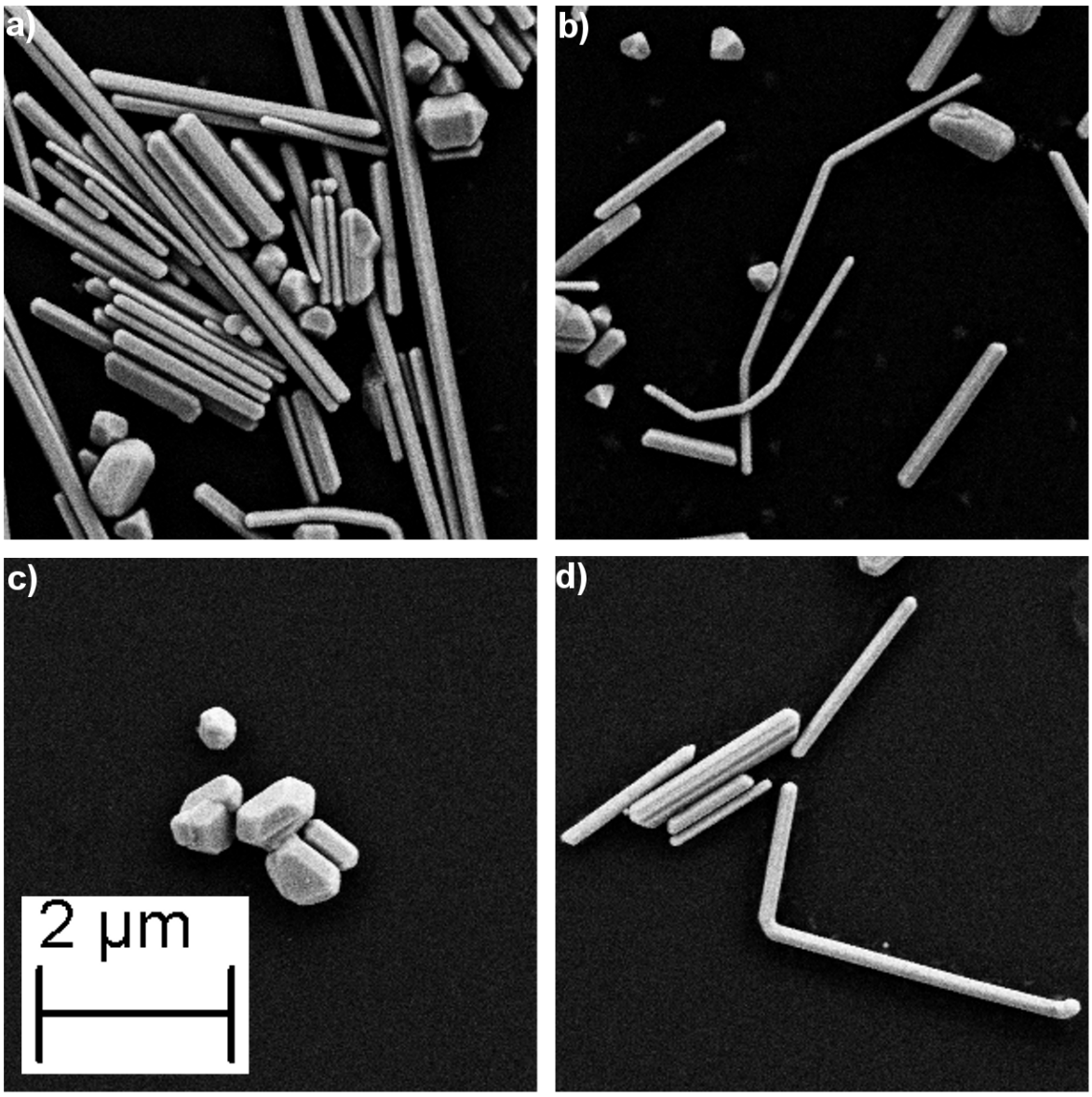

Figure 2: SEM images the various particle geometries. a) straight rods, symmetrical and asymmetrical examples can be easily seen b) curved rods c) spheroidal crystalline particles d) an example of two rod fused together.

The as-received material (Batch # 06226) was highly polydisperse in nature, with particles varying significantly in length and width. Rods are the by far the most common shape observed, with faceted symmetrical rods the most common form, although asymmetrical rods were also observed (Fig 2a). Bent and curved rods were also observed (Fig 2b), with some seemly consisting of two or more straight rods fused together at their ends (Fig 2d).
A sizable population of crystalline spheroidal particles can also be observed (Fig 2c), although it is difficult to ascertain if these are Ag nanoparticles or crystallised components of the suspension media, which is known to contain polyvinylpyrrolidone, an acrylic/acrylate copolymer and polycarboxylate ether.

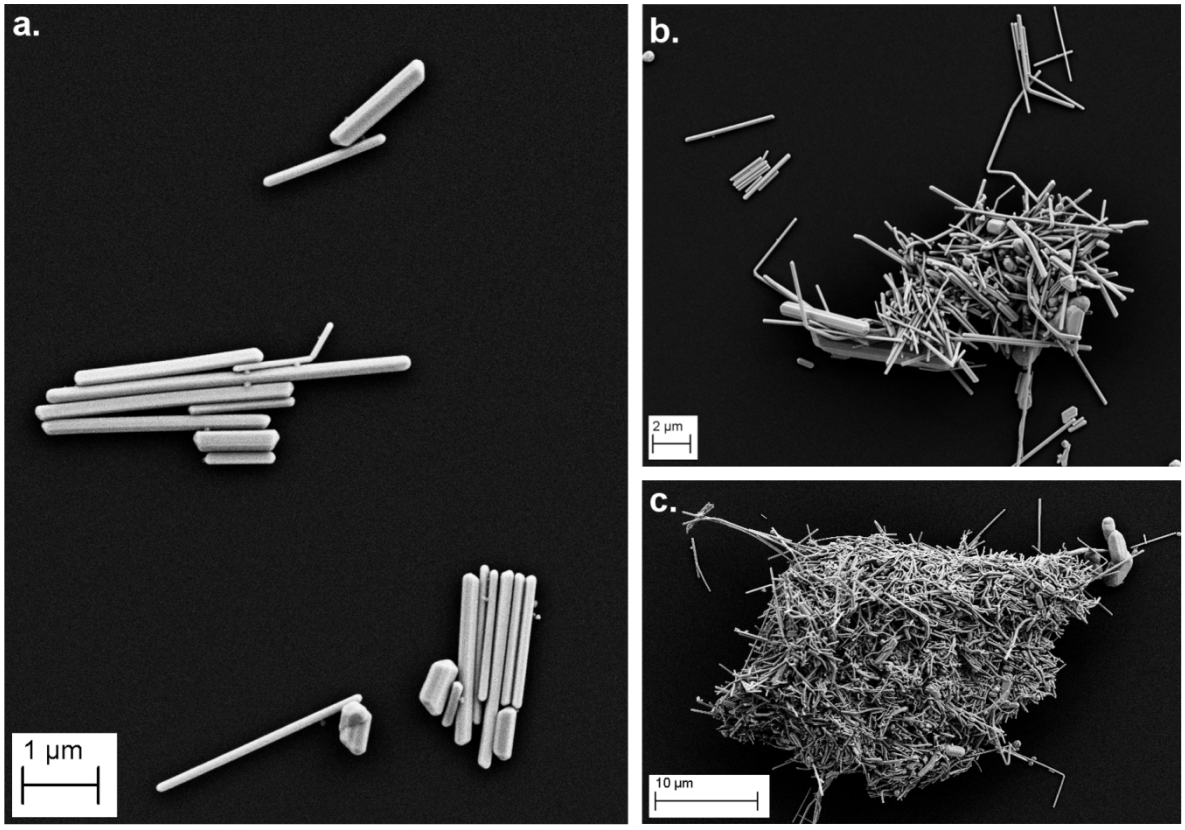

Figure 3: SEM images of agglomerated states of the nanorods a) small loose agglomerates b) larger agglomerates, some individually isolated rod can also be seen c) very large tangled agglomerate

The most common state for the particles was in loose agglomerates of 5-10 particles (Fig 3a), although individually dispersed particles were commonly seen too (Fig 3b). Larger clusters upwards of 10 µm, consisting of tangled masses of hundreds or thousands of particles were also present in low numbers (Fig 3c).

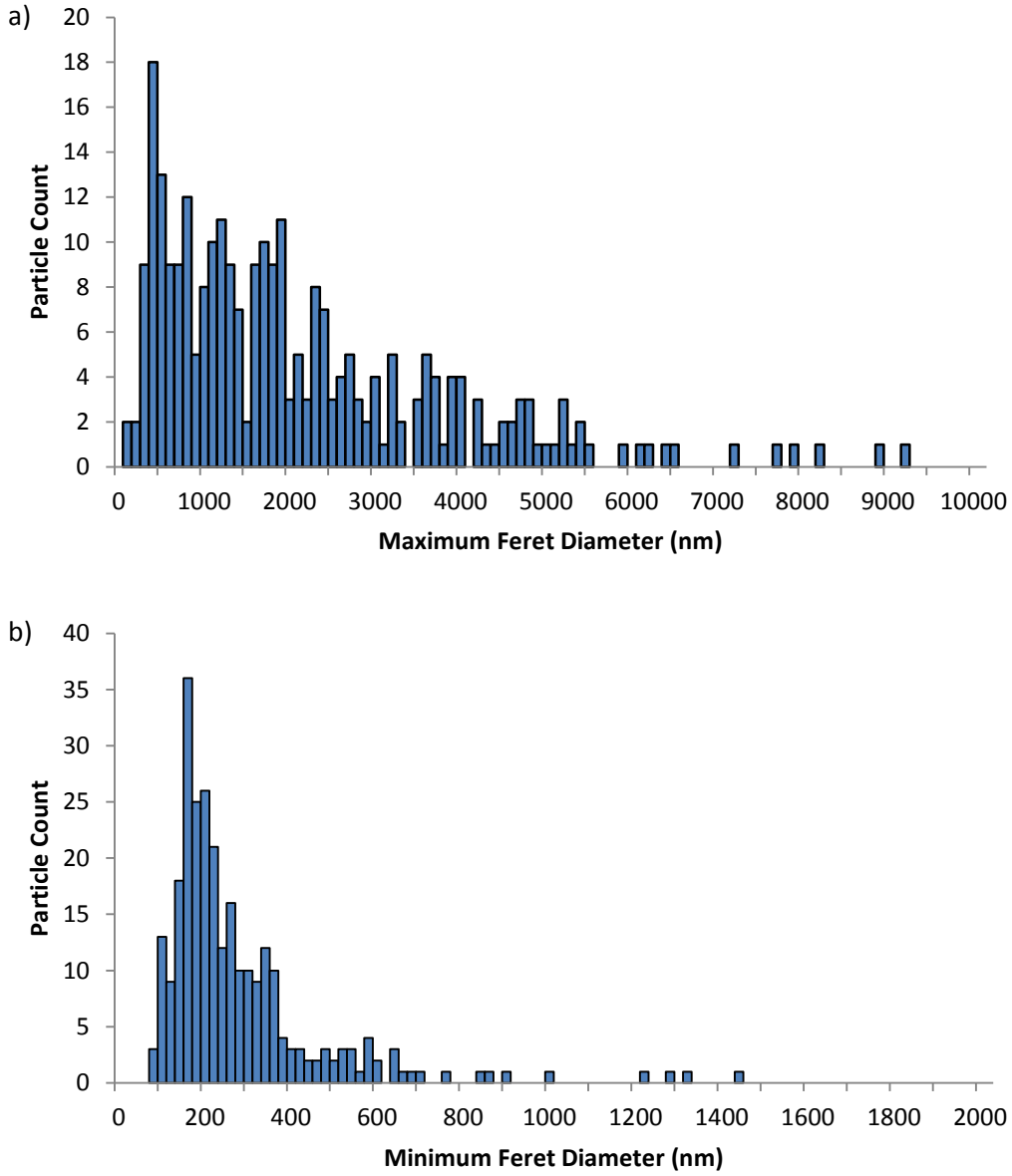

Figure 4: SEM particle diameter distributions. Particle count = 278. a) Feret diameter distribution (bin size = 100 nm), b) minimum feret diameter distribution (bin size = 20 nm)

A total of 278 particles were measured over 5 images (Fig 4). Particle dimensions were defined by the maximum and minimum Feret diameters, which are the maximum and minimum distances between two parallel lines located on the outline of a particle; also commonly known as the "calliper length". As the particles are rods, the maximum and minimum Feret diameters can be considered to give a good estimation of particle length and width. Although in the case of bent or curved rods these measurements will under and overestimate length and width respectively.

The Feret diameter plots (Fig 4) demonstrates the polydisperse nature of NM 302, Maximum Feret diameter (Fig 4a) showing a maximum around the 400- 500 nm range, but with significant proportion of longer rods also present. Minimum Feret diameter (Fig 4b) showed a maximum around 200 nm and a less polydisperse distribution.

Due to uncertainties about the nature of the spheroidal particles present a second dataset was also generated where particles with aspect ratios below 2 were excluded (Fig 5).

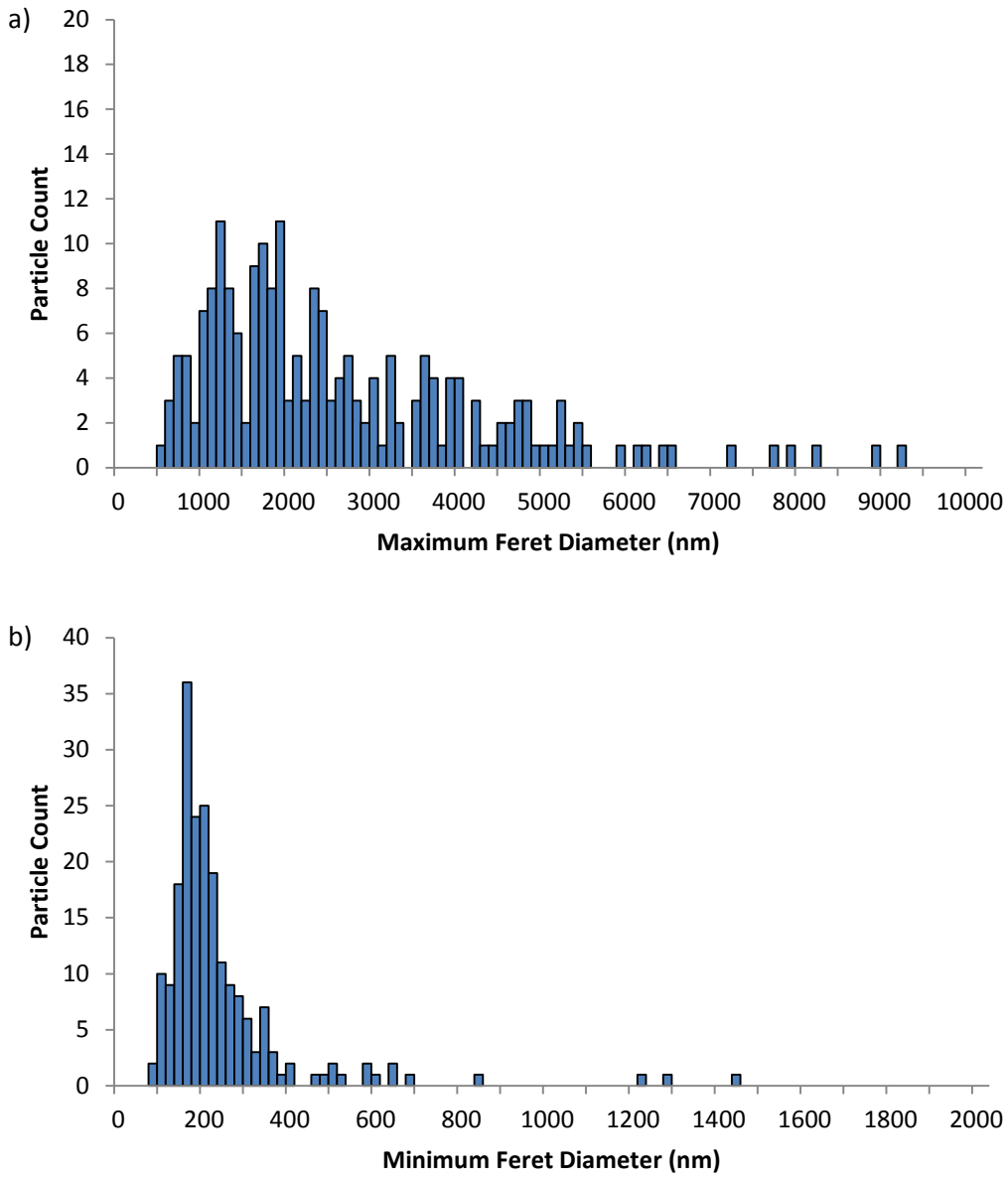

Figure 5: SEM particle diameter distribution, excluding particles with aspect ratios < 2. Particle count = 209. a) Maximum Feret diameter distribution (bin size = 100 nm) b) Minimum Feret diameter distribution (bin size = 20 nm)

The most noticeable difference when excluding spheroidal particles was a significant loss of particles in the 300 - 600 nm range (Fig 5), signifying that the majority of these spheroidal particles were typically a few 100 nm's in size.

Table 2 SEM particle statistics

		Data Set	
		All particles	**Excluding spheroids**
Maximum Feret Diameter (nm)	**Mean**	2077	2594
	±σ	1714	1676
	RSD (%)	83	65
Minimum Feret Diameter (nm)	**Mean**	270	228
	±σ	197	172
	RSD (%)	73	76
Aspect Ratio	**Mean**	11.35	14.71
	±σ	10.20	9.65
	RSD (%)	89.89	65.65

Table 2 summarises the SEM particle sizing results, with the large relative standard deviations (RSD) demonstrating the high polydispersity of the NM 302 material. Comparison of the mean minimum Feret diameter values with those obtained via DCS (Table 1) shows reasonable agreement, especially in the case of the "All particles" data set, where DCS reported number mean particle diameter of 286 nm.

It is interesting to note that most particles measured had significantly different dimensions from the values supplied by the manufacturer, with width being slightly higher and length significantly smaller than the manufacture values of 100 – 200 nm and 5 – 10 µm respectively. Although it should be noted that the small sample populations associated imaging techniques in general, will mean that they are more suitable as a qualitative rather than quantitative tools.

3.1.3 Dynamic light scattering (DLS)

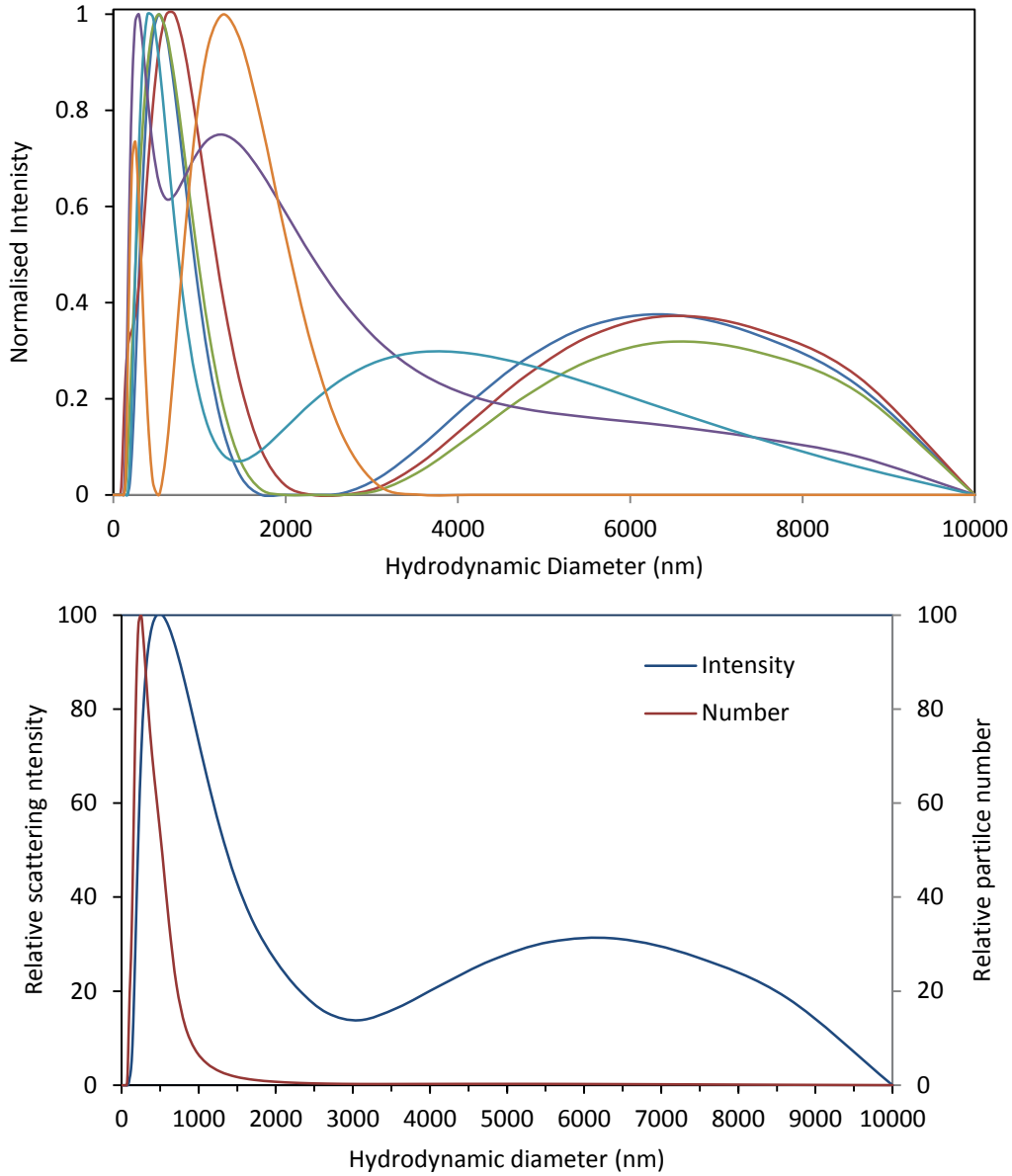

Figure 6: DLS particle diameter distributions for NM 302 (Batch # 06247) a) Scattering intensity distribution of six dispersions b) Averaged intensity and number distributions for six dispersions

Figure 6 shows the DLS particle size distributions NM 302 dispersions. The polydisperse nature of NM302 is again apparent, with large variability between the particle diameter distributions (Fig 6a). Despite the large variation it can be seen that the dispersions typically consist of a primary particle population around 500 - 1000 nm. Inspection of the averaged intensity distribution (Fig 6b) show a primary peak at 458 nm followed by a much broader secondary one extending from ~3 µm to the limit of the instrument (10 µm). The averaged number distribution shows one peak at 255 nm.

Z-average diameters (Table 3); which are based on the intensity distributions, are fairly consistent, reporting an average particle diameter of 499 ± 22.4 nm. This is quite different from the results obtained via DCS and SEM.

Table 3: DLS Z-average particle diameter results. Note PDI here is calculated via the cumulants method as so is not directly comparable to PDI in the DCS results

Sample	Z-Average Diameter (nm)	PDI
1	539.8	0.428
2	480	0.479
3	497.9	0.374
4	480.9	0.48
5	506.7	0.409
6	488.9	0.555
Mean	499	0.454
±σ	22.43	0.064
RSD %	4.49	14.10

It should be noted that DLS is a poor measurement technique for analysis of polydisperse materials such as NM 302, due to large particles scattering significantly more light that smaller ones, which allows small numbers to skew the distribution or mask the signal from smaller particles. This, combined with the poor stability of NM 302 even at low dilutions, was the most likely cause of the large variations in the obtained size distributions.

3.1.4 Scanning mobility particle sizing (SMPS)

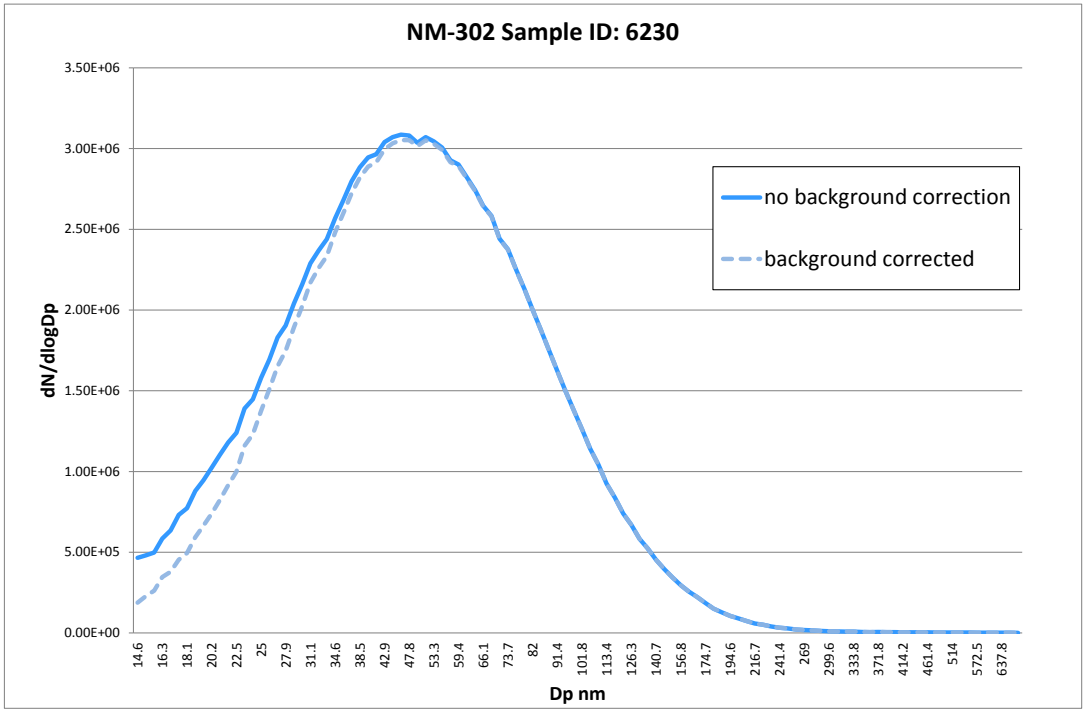

Figure 7: SMPS scan of aerosolised NM 302, with and without background solution correction

Two batches of the NM-302 nano-silver samples were tested (#6230 and #6216) giving similar results; the discussion therefore will be focused on #6230.
From past experience, it is known that even ultra-pure DI water can give significant concentration readings in the SMPS, especially at sizes below 20 nm. For this reason, size distributions of nano-silver-free DI water aerosol were first taken, before adding the nano-silver sample in solution. Hence, a background distribution was established which could easily be subtracted from the sample measurement.

It should be noted that the reported sizes refer to the spherical equivalent electrical mobility diameter the size of spherical charged particles with the same terminal migration velocity in still air as the sample particles, when under the influence of a constant electrical field. As the sample tested here are elongated rods, interpretation of the observed size values is complicated.

Figure 7 shows the SMPS results for #6230. There is a noticeable effect of the background water signal, but only below 30 nm, which in any case does not affect the distribution characteristics significantly. The calculated median size was 48 ± 1.7 nm. This is considerably smaller than results obtained from other techniques, suggesting that the larger particles were not being aerosolised during the measurement process.

3.1.5 X-ray diffraction (XRD)

Traditionally XRD has been used to determine the crystalline structure of materials. However, it can also be used to provide crystallite size by using the Scherrer equation, which is dependent on the width of the peaks seen in the XRD spectrum.

$$\tau = \frac{K\lambda}{\beta cos\theta}$$

τ = the mean size of crystalline domains
K = a dimensionless constant
λ = the X-ray wavelength;
β = the line broadening and FWHM
θ = the Bragg angle.

Table 4: XRD results for NM 302 (Batch # 06275)

Sample	λ (nm)	K	β, 2°	β (rads)	θ, 2°	θ (rads)	cosθ	Crystallite size (nm)
06275	1.54	0.900	0.122	0.00213	37.7	0.658	0.791	82.3

Analysis was carried out on a single sample yielding a crystallite size of 82.3 nm. It should be noted that crystallite size is not equivalent to particle size as particles can consist of multiple crystallites.

3.2 STABILTY

3.2.1 Zeta potential

A common method of determining dispersion stability is through the estimation of zeta-potential values. Zeta potential gives an indication of the electrostatic repulsion forces between particles, in which a large negative or positive zeta potential will mean an increase in this repulsion, thus a more stable dispersion as the particles are less inclined to agglomerate/aggregate. Zeta potential measurements will solely be governed by the electric properties of solid surface in contact with liquid.

Table 5 : Zeta potential results for NM 302 dispersion

Sample	Zeta Potential (mV)
1	-104
2	-106
3	-112
4	-103
5	-114
6	-122
Mean	-110
±σ	7.28
RSD (%)	6.61

Despite the instability of NM 302 dispersions, the zeta potential of the particles was relatively large, with a mean value of -110 ± 7.3 mV. Typically a zeta potential of ± 20 mV is considered enough to prevent particles from aggregating, although this is highly dependent on the presence of surface chemistry and the contents of the dispersing media.

3.2.2 Turbidity

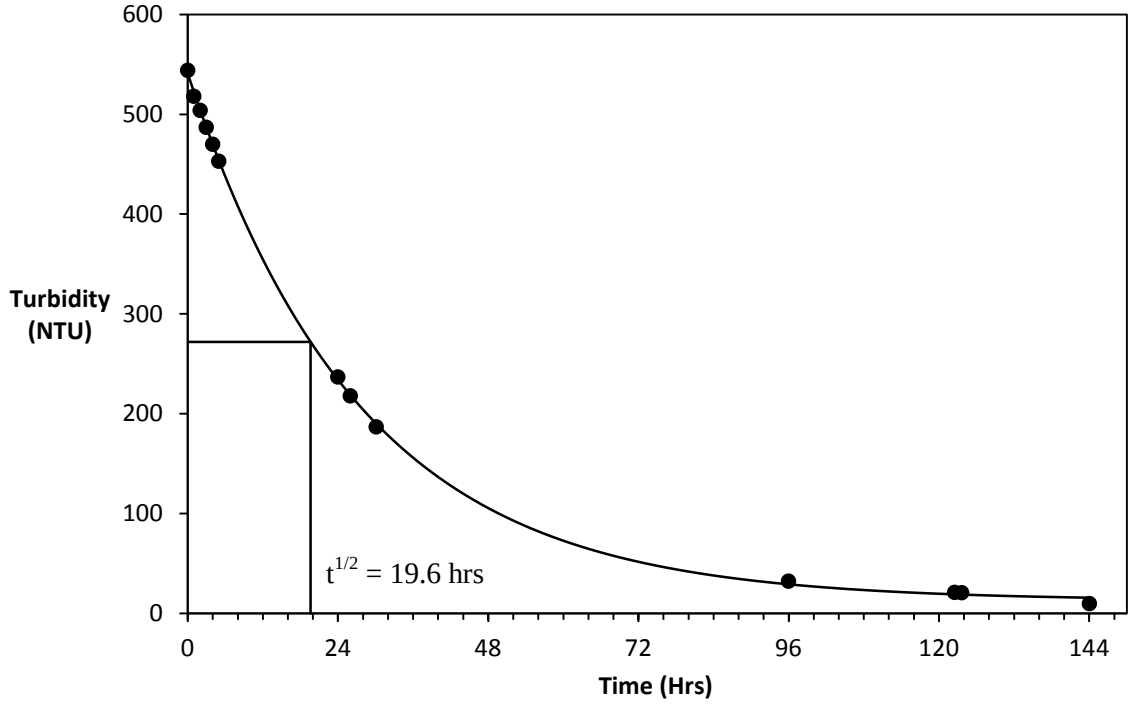

Figure 8 : Plot of change in the turbidity of a NM 302 dispersion (Batch # 06252) with time. The half-life of the decay profile is highlighted.

Following particle sedimentation over time via turbidity measurements can also be used to characterise dispersion stability, with the typically reported measurand, as put forward in the OECD guidelines, the half-life of the decay. Half-life measurements here will not only be governed by the surface charge property but also other contributory factors such as sedimentation kinetics which is linked to particle size and density. Figure 8 shows the decrease in turbidity with time of a NM 302 dispersion, with a half-life of 19.6 hours was recorded. This is moderately stable when compared to the nanomaterials studied previously under PROSPEcT which ranged from 3.6 to 67.3 hours depending on nanomaterial and dispersing media.

3.2.3 Redox potential

Table 6: Redox potential values for NM302 dispersion (Batch # 06247).

Measurement	T (^{o}C)	Redox potential - corrected to SHE (mV)
1	21.7	510.0
2	21.6	509.0
3	21.7	509.0
4	21.6	508.0
5	21.6	508.0
6	21.8	507.0
Mean	21.7	508.5
±σ	0.1	0.96
RSD (%)	0.3	0.19

As indicated in the OECD guidelines, redox potential (ORP) measures the potential difference across two electrodes: a Pt electrode against a double junction Ag/AgCl reference electrode, when immersed in the nanomaterial dispersion. Table 6 shows the redox potential results for NM 302, and average value of 508.5 ± 0.96 mV was recorded. This was significantly larger than the other NM series tested under PROSPEcT, where values in the range of 380-430 mV were obtained, dependant on nanomaterial and dispersing media.

The ORP values reported here are not specific to a single chemical species and thus represent an aggregate oxidization-reduction of all species that can interact at the platinum working electrode.

3.2.4 Reactive oxygen species (ROS)

This study was conducted to determine the ability of the nanomaterials to generate reactive oxygen species (ROS), including radicals, under photo-catalytic conditions and Ag nanoparticles specifically are theorised to generate ROS via SPR induced effects.[2] KI was used as a source of iodide anions, which can act as molecular probes for ROS. When the iodide anions are oxidized, yellow I_3- is formed, which exhibits an optical absorption peak at 352 nm, the concentration of I_3- can be determined using its molar extinction coefficient ($\varepsilon = 26000$ $Lmol^{-1}cm^{-1}$), although relating this back to ROS concentrations is difficult for complex media where other components may compete with the iodide anions for ROS. NM 302 dispersions with KI were used as positive control; NM 302 dispersant with KI was used as a negative control. NM 302 dispersion without KI was also studied to investigate if the nanorods themselves could affect the absorbance

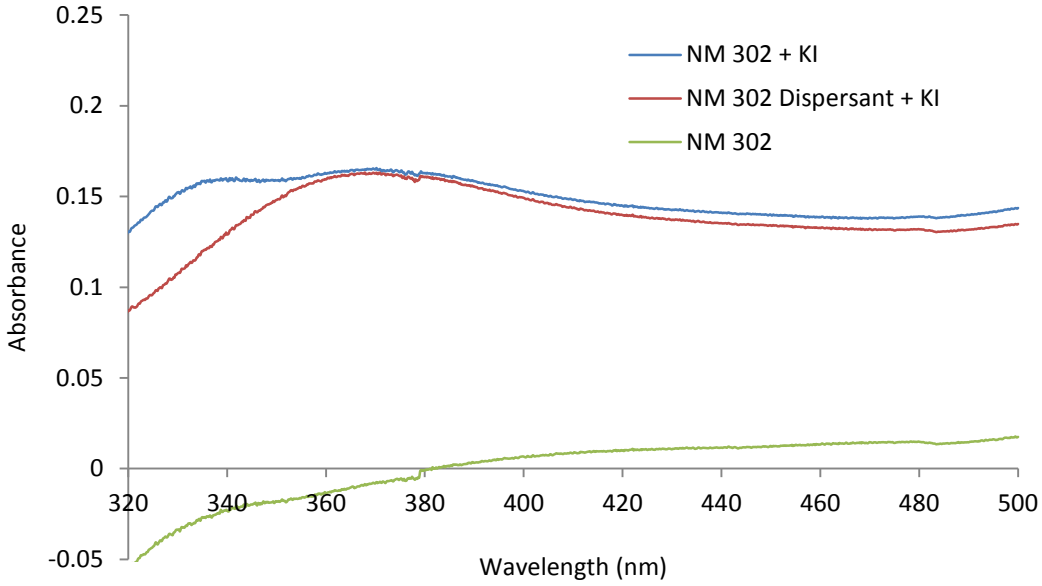

Figure 9: UV-Vis adsorption spectra for ROS. Spectra are the average of six measurements. NM 302 dispersions were from batch # 06247

Both the positive and negative controls produced I_3- (Fig 9) as evidenced by the increased absorption and a change in colour, implying that one or more of the components in NM 302 dispersant is capable of producing ROS, although the expected 352 nm peak was seemingly masked by other components. The UV irradiated NM 302 dispersion produced negative adsorption values at low wavelengths, suggesting that one or more of the dispersant components undergo photo-catalysed reactions.

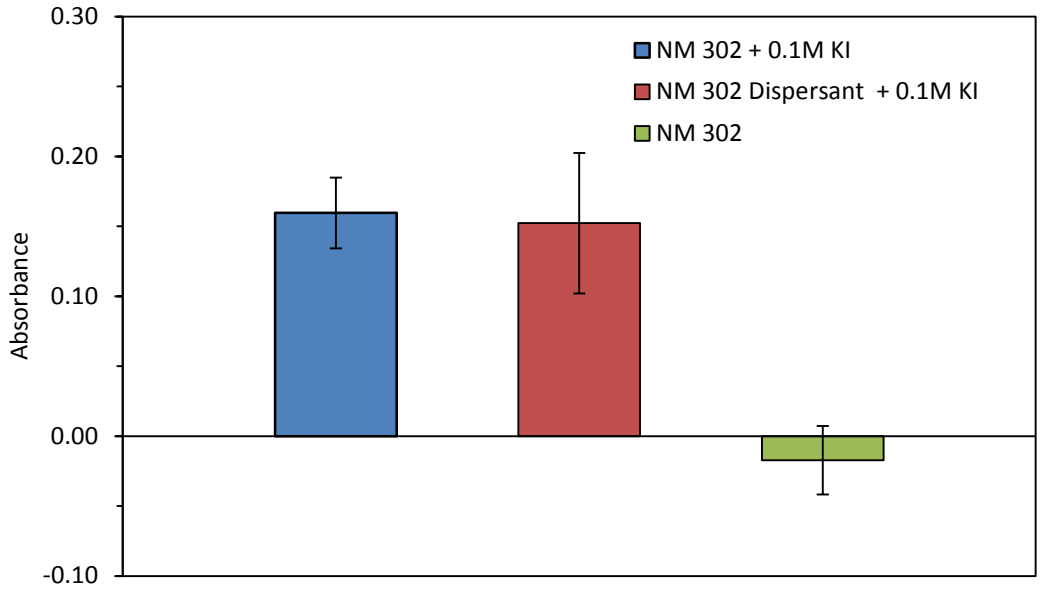

Figure 10: Absorbance at 352 nm. Values obtained from six measurements per sample.

Figure 10 shows the absorbance values at 352 nm for the various tested samples. As expected the samples with KI produced higher absorption values, and were comparable to those obtained from previously measured NM series samples in PROSPEcT, where absorbance values of 0.1 - 0.2 were reported for most samples in complex media. Although the difference between the absorbance values from the NM 302 and NM 302 dispersant samples was very small (5%) suggesting the Ag nanorods were not the main factor in I_3- formation.

4. CONCLUSIONS

Various physico-chemical characteristics of the NM 302 silver nanorod reference material have been reported.

Although characterisation has been carried out, there is a need to appreciate analytical challenges associated with the characterisation of this sample. The instability of the supplied samples and complex nature of dispersant made the many of the characterisation techniques difficult to perform.
Strange results associated with zeta-potential, DLS particle size measurements and ROS were a particular, but not unexpected, issue, as these techniques are sensitive to sample stability, size polydispersity and dispersing media. Analytical challenges associated with nanomaterial characterisation associated with highly polydisperse sample have been previously reported and are well documented.[3]

1. Fabrega, J.; Tantra, R.; Amer, A.; Stolpe, B.; Tomkins, J.; Fry, T.; Lead, J. R.; Tyler, C. R.; Galloway, T. S., Sequestration of Zinc from Zinc Oxide Nanoparticles and Life Cycle Effects in the Sediment Dweller Amphipod Corophium volutator. *Environ. Sci. Technol.* **2011,** *46* (2), 1128-1135.
2. Zhang, W.; Li, Y.; Niu, J.; Chen, Y., Photogeneration of Reactive Oxygen Species on Uncoated Silver, Gold, Nickel, and Silicon Nanoparticles and Their Antibacterial Effects. *Langmuir* **2013,** *29* (15), 4647-4651.
3. Tantra, R.; Shard, A., We need answers. *Nat. Nanotechnol.* **2013,** *8* (2), 71-71.